Theor Chem Acc (2002) 107:291–303
DOI 10.1007/s00214-002-0331-4

Theoretical
Chemistry Accounts

Regular article

Some thoughts about the stability and reliability of commonly used exchange–correlation functionals – coverage of dynamic and nondynamic correlation effects

Victor Polo, Elfi Kraka, Dieter Cremer

Department of Theoretical Chemistry, Göteborg University Reutersgatan 2, 41320 Göteborg, Sweden

Received: 8 November 2001 / Accepted: 30 January 2002 / Published online: 8 April 2002

Abstract. The self-interaction error (SIE) of commonly used density functional theory (DFT) exchange functionals mimics long-range (nondynamic) pair correlation effects in an unspecified way. Slater exchange suffers from a larger SIE and, therefore, covers more nondynamic correlation effects than Becke exchange, which is the reason why exchange–correlation (XC) functionals based on Slater exchange lead to stabler restricted DFT solutions than those based on Becke exchange. However, the stability of an XC functional does not guarantee higher accuracy. On the contrary, if system-specific nondynamic correlation effects have to be introduced via the form of the wave function, these will be suppressed by nondynamic correlation effects already covered by the exchange functional. Hybrid functionals suffer less from the SIE and, therefore, cover a smaller number of nondynamic electron correlation effects. Accordingly, they are better suited when nondynamic electron correlation has to be introduced by the form of the wave function. It is shown that, for example, broken-symmetry unrestricted DFT calculations are more accurate when carried out with B3LYP than BLYP contrary to claims made in the literature.

Key words: DFT – Self-interaction error – SIC-DFT – Exchange effects – Correlation effects – Long-range correlation

1 Introduction

Despite the enormous success of density functional theory (DFT) [1, 2, 3] in the realm of chemistry during the last 15 years, [4] there are still well-known shortcomings of DFT, which hamper its application in a more predictable way. In general, the deficiencies of DFT can be traced back to the approximate nature of the commonly used exchange–correlation (XC) functionals [5–18]. They have been constantly improved from the original local density approximation (LDA) functionals [5, 6, 7] to the better performing general gradient approximation (GGA) functionals, [8, 9, 10, 11] then to the (partially empirically adjusted) hybrid functionals [12, 13, 14, 15, 16] and finally to the kinetic energy density functionals [17, 18] that improve in particular exchange. However, even the best XC functionals available today are still approximate and, therefore, cannot guarantee that any new type of electronic system, single-reference or multireference in nature, is correctly described by the Kohn–Sham (KS) determinant.

In this work, we show that the self-interaction error (SIE) of approximate XC functionals [19–28] has a major impact on the performance of standard DFT methods. The SIE, although an error in nature, is preferentially responsible for the stability of XC functionals. The internal and external stability of a restricted DFT (RDFT) description of a given electronic system can be determined with the help of stability matrices [29, 30]. For example, in the case of a dissociating molecule *A*-*A* the RDFT solution becomes externally unstable at a particular distance $r_b(A\text{–}A)$ where the RDFT and unrestricted DFT (UDFT) solutions bifurcate, the latter being lower in energy than the former. This is indicated by the fact that the external stability matrix possesses one negative eigenvalue, λ, indicating a breaking of the constraint $\psi_\alpha = \psi_\beta$. The more negative λ is, the larger is the observed instability. The corresponding eigenvector leads outside the restricted subspace, thus yielding an UDFT energy lower than the RDFT energy [30, 31]. For a given value of $r(A\text{–}A) > r_b$ (*A*-*A*), the energy lowering, $\Delta E(U-R)$, can also be used to assess the instability of the RDFT solution [31].

In a previous investigation, Gräfenstein et al. [31] found that in general LDA functionals are more stable than GGA functionals and the latter in turn are more stable than hybrid functionals. The differences $\Delta E(U-R)$ increase parallel to this trend. The general understanding is that a DFT solution is stabler, the more correlation effects are covered by the XC functional in

Correspondence to: D. Cremer
e-mail: dieter.cremer@theoc.gu.se

question. There are considerations in the way that LDA functionals cover more correlation effects than GGA functionals and that the admixture of Hartree–Fock (HF) exchange leads to larger instability of DFT because HF is always less stable than DFT in practical applications [29, 30, 31].

It is well-known that at the HF level of theory, an extension of the basis set increases the stability of the R solution. This holds also for DFT as is reflected by the calculated stability parameters λ and the differences $\Delta E(U-R)$, although normally the changes are relatively small [31].

It has been argued that with increasing stability of an XC functional more reliable DFT descriptions are obtained [32, 33]. Following this argument, the conclusion could be drawn that the LDA functionals provide the most reliable descriptions, which is certainly not true. Nevertheless, it seems to be generally accepted that the stability of a GGA functional such as BLYP compared to that of a hybrid functional such as B3LYP suggests that the former rather than the latter should be used in cases where the stability of the XC functional might matter.

In this work, we investigate the relationship between the SIE and the stability of a given XC functional. It is shown that the SIE of a LDA or GGA exchange functional mimics long-range (nondynamic) electron correlation effects and increases in this way the stability of the corresponding DFT method. We further show that the stability of an XC functional is not necessarily a reliable indicator for its performance. On the contrary, it might disguise shortcomings of the DFT approach as, for example, an unsuitable double counting or a suppression of nondynamic electron correlation effects that one wants to include via the form of the wave function. By analyzing this situation, we demonstrate that it is better to use a hybrid functional such as B3LYP rather than a GGA functional such as BLYP because hybrid functionals by their construction largely avoid a suppression of correlation effects.

The results of this investigation are presented in the following way. The computational methods applied in this work are described in Sect. 2 We show how nondynamic electron correlation effects are included into DFT via the SIE of the exchange functional in Sect. 3. In Sect. 4, the question of a double counting of nondynamic electron correlation is considered and in Sect. 5 the question whether there is a need for generally applicable self-interaction-corrected (SIC) DFT method.

2 Computational methods

Electron correlation leads to the effective separation of n-electron clusters in the available atomic or molecular space. The most important electron correlation effects are found for $n = 2$ or 3, while for higher n-electron clusters disconnected correlation effects involving m-electron ($m < n$) clusters are important. To simplify the discussion, we focus in this work on electron-pair correlation effects, in particular left–right, angular, and in–out correlation. These effects are easy to visualize, while higher-order correlation effects occur simultaneously with lower-order effects and, therefore, are more difficult to separate from the much stronger pair correlation effects. The degree of electron-pair correlation is assessed with the help of the electron density distribution, $\rho(\mathbf{r})$. By calculating difference electron density distributions, $\Delta\rho(\mathrm{A,B}) = \rho(\text{method A}) - \rho(\text{method B})$, for a series of wave function theory (WFT) methods with well-defined electron correlation effects, it is possible to set up a qualitative order of increasing pair correlation effects [34, 35, 36, 37].

Terms describing pair correlation effects were originally defined in connection with multiconfigurational self-consistent-field (SCF) calculations, i.e. for nondynamic (long-range) electron correlation; however, they are equally used when describing dynamic (short-range) electron correlation because both long-range and short-range correlation can lead to similar changes in $\rho(\mathbf{r})$. If these changes are made visible by using a suitable reference density, it will not be possible without additional investigations, for example, of the XC hole, to identify left–right separation of negative charge as a short-range or a long-range correlation effect. This has to be considered when discussing the difference density distributions calculated in this work.

In the second step, we compare the electron density distributions generated by commonly used XC functionals with those of suitable WFT reference densities containing specific electron correlation effects. In this way, we identify correlation effects covered by a given XC functional where, again with the help of difference density techniques, the influence of the exchange functional is separated from that of the correlation functional.

Special attention is given to the SIE of the DFT exchange functionals. Actually, correct DFT must fulfill Eqs. (1), (2), (3) and (4), which give the electron interaction energies and the interaction potentials for the limit of a one-electron system. In such a case, the electron density distribution is equal to the spin density distribution, $\rho_\sigma(\mathbf{r})$, which for $\sigma = \alpha$ obeys the conditions $\int \rho_\alpha(\mathbf{r})\mathrm{d}\mathbf{r} = 1$ and $\rho_\beta(\mathbf{r}) = 0$.

$$E_\mathrm{J}[\rho] + E_\mathrm{X}[\rho_\sigma, 0] = 0 \ , \tag{1}$$

$$E_\mathrm{C}[\rho_\sigma, 0] = 0 \ , \tag{2}$$

$$\upsilon_\mathrm{J}([\rho];\mathbf{r}) + \upsilon_\mathrm{X}^\sigma([\rho_\sigma, 0];\mathbf{r}) = \text{constant} \ , \tag{3}$$

$$\upsilon_\mathrm{C}^\sigma([\rho_\sigma, 0];\mathbf{r}) = 0 \ . \tag{4}$$

Clearly, a single electron does not interact with itself and, therefore, the self-repulsion energy of the electron contained in $E_J[\rho]$ has to be canceled by the self-exchange energy $E_\mathrm{X}[\rho_\sigma, 0]$ ($\rho_\sigma = \rho_\alpha$ and $\rho_\beta = 0$) covered by the exchange functional (Eq. 1). Equation (2) clarifies that a single electron does not possess any self-correlation energy and Eqs. (3) and (4) make sure that the single electron moves under the influence of the external potential, $\upsilon_\mathrm{ext}(\mathbf{r})$, of the atomic nuclei rather than the self-Coulomb, self-exchange, and self-correlation potentials υ_J, υ_X, and υ_C, respectively. LDA and GGA exchange functionals violate Eqs. (1) and (3), while most correlation functionals (exception LYP) violate Eqs. (2) and (4). SIC-DFT methods [21, 22, 23, 24, 25, 26, 27, 28] are designed to correct approximate XC functionals in such a way that Eqs. (1), (2), (3) and (4) are restored. In the following, we denote self-interaction corrected exchange and correlation functionals as SIC-X and SIC-C functionals leading to SIC-DFT methods. With regard to the SIE, we distinguish between X-SIE and C-SIE, respectively.

For the purpose of calculating the SIE of commonly used XC functionals the method developed by Perdew and Zunger was employed [7, 21, 22]. The calculation can be carried out in a single-step SIC-DFT procedure to estimate the magnitude of the SIE or within a SCF-SIC-DFT procedure [24, 27] to calculate molecular properties such as the electron density distribution. The Perdew–Zunger method has the advantage of retaining the size-extensivity of DFT [22]. It leads, however, to an orbital-dependent functional and the results are no longer invariant with regard to rotations among the occupied orbitals. Another problem inherent in the Perdew–Zunger approach is that the lowest SCF energy can only be obtained by minimizing the energy for localized orbitals [24]. Localization of the orbitals of a σ–π system leads to bent bonds and, accordingly, SCF-SIC-DFT densities are no longer comparable with DFT or WFT densities. One can circumvent this problem by localizing σ and π orbitals separately and rotating the localized orbitals only within a given set. In this way, only a part of the SIE is

recovered (about 80% for molecules with a double bond [28]); however, the comparison of SCF-SIC-DFT and DFT densities becomes meaningful, in particular as this is done in a qualitative rather than a quantitative way.

Small molecules representing typical bonding situations were investigated at the SCF-SIC-DFT level of theory, where we present here just the results for N_2 in its ground state at the experimentally determined bond length, r_e of 1.098 Å [38]. Reference densities were calculated using standard HF, Møller–Plesset (MP) [39, 40], and coupled–cluster (CC) theories [40, 41, 42, 43, 44] with unfrozen core and analytical energy gradients [35], where all MP and CC densities were calculated as response densities using standard procedures [34, 35].

The DFT functionals employed reach from LDA to GGA and hybrid functionals [37]. SVWN [5, 6], SVWN5 [5, 6], and the SPL [5, 7] functionals were used as typical LDA functionals, the BLYP [8, 10], BPW91 [8, 11], PW91P91 [11], and BP86 [8, 9] functionals as typical GGA functionals, and the BH&H [12], B3LYP [13], B1LYP [14, 15], and the mPW1PW91 [16] functionals as typical and most often used hybrid functionals. The electron interaction effects caused by X-SIE were obtained by comparing SIC-X calculations with exchange-only (X-only) calculations. The SIC-C was investigated in different ways; namely, by comparing SIC-XC with SIC-X densities, with the help of the difference density generated from HF + SIC-C and HF calculations, and from the difference density distribution defined by $[\rho(\mathrm{XC}) - \rho(\mathrm{X})] - [\rho(\mathrm{HF}+\mathrm{C}) - \rho(\mathrm{HF}+\mathrm{SIC\text{-}C})]$. These procedures use different orbitals and so they should lead to differing SIC-C densities; however, the difference density plots obtained by the three approaches agree qualitatively, so in the following discussion there is no need to distinguish between SIC-C density distributions obtained in different ways [28].

All the calculations were carried out with Dunning's cc-pVTZ basis set, which corresponds to a (10s5p2d1f) [4s3p2d1f] contraction [45]. The calculations were done with the quantum chemical program packages COLOGNE2001 [46], GAUSSIAN98 [47], and ACES II [48].

3 Nondynamic correlation effects covered by the exchange functional

The difference electron density distributions obtained with correlation-corrected WFT methods and X-only DFT calculations are shown in Fig. 1 for the ground state of the N_2 molecule. The difference density $\Delta\rho(\mathrm{MP2,HF}) = \rho(\mathrm{MP2}) - \rho(\mathrm{HF})$ (Fig. 1a) reveals how the HF density changes when electron correlation effects are included into the calculation. Electron-pair correlation is introduced at the MP2 level of theory by double (D) excitations, which transfer density out of the bond region toward the N atoms (left–right correlation). Also, density is shifted from the inner region of the electron lone pairs of N (arranged along the molecular axis) to the outer regions (in–out correlation). Obviously, there is also considerable angular correlation because of the increase of the electron density in the regions of the $2p\pi$ orbitals of the N atoms (Fig. 1a).

At the MP3 level of theory left–right, in–out, and angular correlation are decreased as is shown by the difference electron density distribution $\Delta\rho(\mathrm{MP3,MP2}) = \rho(\mathrm{MP3}) - \rho(\mathrm{MP2})$ (see Fig. 1b). There is a transfer of negative charge from the valence regions of the atoms back into the bond region and from the outer regions back to the inner regions of the lone pairs. Hence, the strong pair correlation effects obtained at the MP2 level are reduced at the MP3 level of theory. It is known that MP3 corrects the exaggeration of pair correlation obtained at the MP2 level by a coupling of the D excitations [40].

At each higher level of WFT, the pair correlation effects are further fine-tuned, which becomes visible by analyzing the relevant difference densities. For N_2 and other small molecules, one finds that MP and CC methods can be ordered qualitatively in a series (Fig. 2) according to their ability to separate the two electrons of an electron pair (bond or lone pair) by left–right, in–out, and angular correlation, where the latter effects are difficult to separate from the former.

The difference density distributions generated for the WFT methods reveal that MP4(SDQ) covers more pair correlation effects than MP3 but still exaggerates pair correlation, which is corrected at the CCSD level of theory because infinite-order effects in the SD space exclude any exaggeration of pair correlation effects. Three-electron correlation as included by triple (T) excitations at the MP4 level of theory separates electrons in the triple bond of N_2 more effectively {Fig. 1c: $\rho(\mathrm{MP4}) - \rho[\mathrm{MP4(SDQ)}]$}; however still not as strongly as at the MP2 level of theory [Fig. 1d: $\rho(\mathrm{MP4}) - \rho(\mathrm{MP2})$]. We note in connection with this that the mechanism of electron correlation is basically different as soon as T excitations are included, but for reasons of simplicity, we continue to consider just the degree of left–right or in–out separation of negative charge as caused by T excitations. Figure 1a–d confirm that pair correlation effects are strongly exaggerated by just using uncoupled D excitations [40].

At the MP4 level of theory, the separation of negative charge is still overestimated and is corrected when infinite-order correlation effects are also included into the T space. CCSD(T) [44] covers about 70% of these effects [49] and, by this, provides a more balanced account of the separation of negative charge by left–right or in–out correlation. At CCSD(T), pair correlation is less than found at either the MP2 or MP4 levels of theory (Fig. 2).

When the electron density distribution generated at the X-only level of theory is compared with that obtained at the HF [Fig. 1e: $\rho(\mathrm{B\text{-}only}) - \rho(\mathrm{HF})$], MP$n$ or CC levels of theory, strong pair correlation effects are also observed. Actually, left–right separation of charge is stronger at the B-only level of theory than at the MP2 level and this is once more increased at the S-only level of theory [Fig. 1f: $\rho(\mathrm{S\text{-}only}) - \rho(\mathrm{B\text{-}only})$]. A different quality in pair correlation effects seems to be reproduced by the X functionals than by MP or CC methods. We show in the following that in the former case correlation effects are actually (long-range) nondynamic rather than (short-range) dynamic and that they are caused by the SIE of the X functionals used.

The self-interaction of electrons is largest in those regions where the density is large, i.e. where the occupied orbitals possess large amplitudes; hence, strong self-interaction effects of electrons occur in the core, bond, and lone-pair regions, which leads to a reduction (by stronger Coulomb self-repulsion) or an increase of the density (by stronger self-exchange). The changes in the electron density caused by HF self-exchange are reflected in Fig. 3. Since HF self-repulsion is exactly

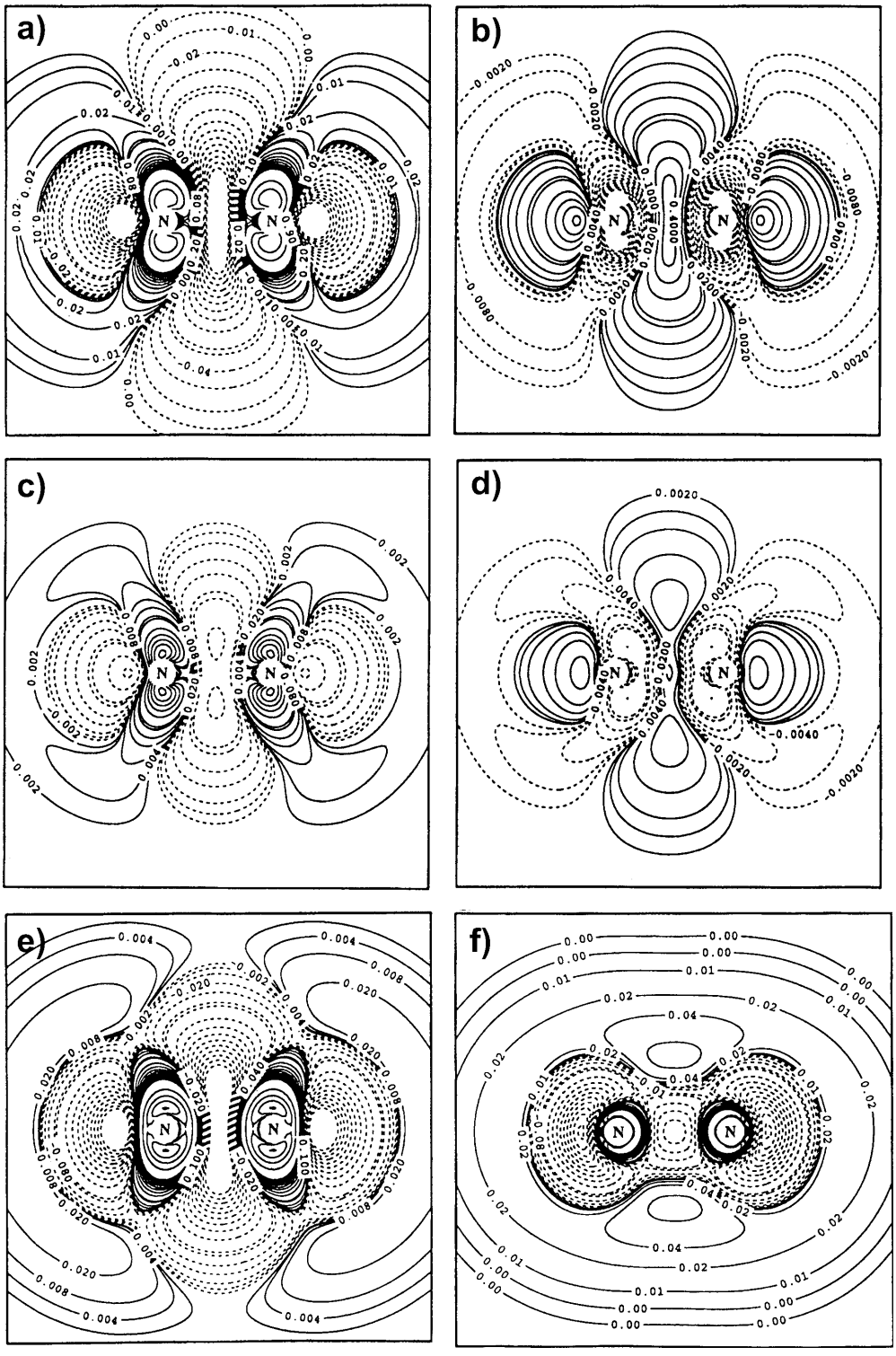

Fig. 1a–f. Contour line diagram of the difference electron density distribution $\Delta\rho(\mathbf{r})=\rho(\text{method1})-\rho(\text{method2})$ of $N_2, {}^1\Sigma_g^+$ calculated with the cc-pVTZ basis at the experimental geometry. The *solid* (*dashed*) contour lines are in regions of positive (negative) difference densities. The reference plane is the plane containing the two nuclei. The positions of the atoms are indicated. The contour line levels have to be multiplied by the scaling factor 0.01 and are given in e bohr^{-3}. **a** MP2–HF, **b** MP3–MP2, **c** MP4–MP4(SDQ), **d** MP4–MP2, **e** B only–HF, **f** S only–B only

canceled out by HF self-exchange, the corresponding diagram reflecting the changes in the electron density caused by self-repulsion is just the mirror image of Fig. 3a, i.e. the difference density of Fig. 3a has to be multiplied by -1.

The Coulomb self-repulsion of the electrons at the HF level removes density out of the bond and lone-pair regions into the valence regions of the atoms and the van der Waals regions. HF self-exchange has just the opposite effect, i.e. it transfers density back into the bond and lone-pair regions (Fig. 3a) and so the two effects cancel each other exactly. If approximate XC functionals are employed, Coulomb self-repulsion will be larger than self-exchange in the bond region. Accordingly, density is removed artificially out of the bond regions by the resulting X-SIE, thus simulating left–right and other pair

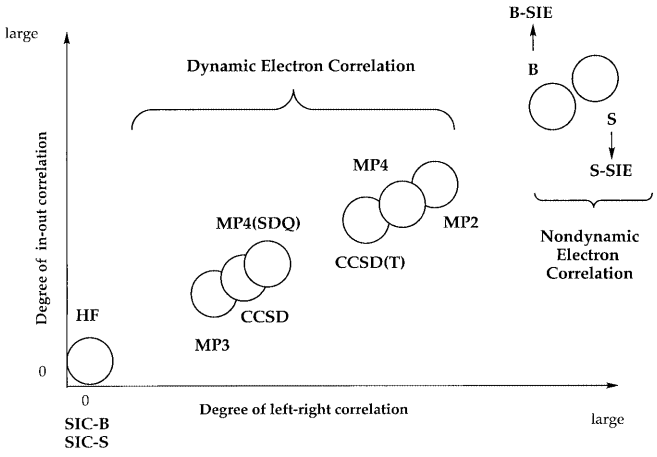

Fig. 2. Schematic representation of the degree of left–right and in–out pair correlation effects for different wave function theory (*WFT*) and density functional theorem (*DFT*) methods [41]. For different molecules the sequence of methods may change somewhat, which is indicated by overlapping areas

correlation effects. This can be illustrated by plotting the density changes resulting from the B-SIE functional as reflected by the difference density $\Delta\rho(\text{B-SIE}) = \rho(\text{B-only}) - \rho(\text{SIC-B})$ (Fig. 3b). The corresponding changes in the electron density are closely related to those caused by MP2 when using the HF electron density distribution as reference (Fig. 1a). In the following we show that the MP2 density covers short-range, dynamic correlation effects, while the B-SIE density represents long-range, nondynamic electron correlation effects.

The approximate DFT exchange hole is, similarly as the total XC hole, by construction localized, spherically symmetric, and depends on the position of the reference electron. Schematic one-dimensional representations of HF, SIC-DFT, and DFT exchange holes are given for H_2 (A = H) in Fig. 4. Two positions of the reference electron are considered; namely, at the bond midpoint of H_2 and at one of the nuclei. SIC-DFT should lead to an exchange hole that is similar or, assuming the same density, identical to the HF exchange hole. In the case of H_2, the latter is identical to the self-exchange hole and equal to $-\rho(\mathbf{r})$ given by the σ_g orbital density. Hence, the SIC-DFT exchange hole is delocalized and is independent of the position of the reference electron (Fig. 4a, b). For molecules with A not being hydrogen, the structure of the SIC-DFT exchange hole becomes more complicated and depends on the position of the reference electron. Nevertheless, for the latter being at the bond midpoint the structure should be similar to that shown in Fig. 4a for H_2. Also, when the reference electron moves in the direction of one nucleus A features of the SIC-DFT exchange hole should resemble those shown in Fig. 4b for the SIC-DFT exchange hole of H_2. Hence, conclusions drawn for H_2 should be also valid for N_2 or other A_2 molecules.

In general, correct exchange holes tend to be delocalized (Fig. 4) as was first pointed out by Slater [5, 50] and later emphasized in particular by Becke [51], Gritsenko et al. [52], and Schipper et al. [53]. However, one should consider that with the reference electron being at a nucleus A ($A >$ He) a HF or SIC-DFT exchange hole can also be localized because of the fact that core electrons are localized at a nucleus. Hence, the tendency of exchange holes to delocalize corresponds to situations where the reference electron is in the bond region probably occupying the bond orbital. Then, the negative of the bond orbital density will shape the self-exchange hole similarly as in the case of the H_2 molecule and the self-exchange hole, in turn, will strongly influence the structure of the total exchange hole by imposing the delocalized form of the bonding orbital on it.

One can relate the structure of the exchange hole to the density or difference density distributions shown in this work considering that both describe correlation effects. The exchange hole has hardly been used for this purpose in the case of molecules, probably because one expects that only a large (actually, infinite) number of positions of the reference electron can provide a complete description of electron correlation. In practice, however, it is sufficient to consider just a few positions for the reference electron; namely, those that are interesting for the bond or the lone-pair electrons. For example, the structure of the HF exchange hole can be connected in this way to the sum of HF self-exchange (Fig. 3a) and HF interelectronic exchange reflected by the difference density distribution $\Delta\rho(\text{exchange}) = \rho(\text{HF}) - \rho(\text{Hartree})$ (Fig. 3c).

Interelectronic exchange interactions are small in the core regions, in the bond region, and in the van der Waals regions because there is little chance of finding two electrons of the same spin either because of spin-coupling of electrons or because of a low electron density. Exchange interactions are, however, large in the valence region (maximally four electrons of the same spin can be found there for N or other atoms from the first two rows of the periodic table) or in those regions where σ and π density of the N $\equiv$ N bond can penetrate each other, thus enhancing the possibility of finding electrons with the same spin. In all those region where exchange interactions are large, Coulomb repulsion is effectively reduced, thus leading to an increase of electron density as shown in Fig. 3c.

Inspection of the difference density distributions reflecting the effects of interelectronic SIC-B and SIC-S exchange reveals that they qualitatively possess the same features. Differences are made visible by the distributions $\rho(\text{SIC-X}) - \rho(\text{HF exchange})$ (X = B and S) shown in Fig. 3d and e. Both SIC-B and SIC-S exchange lead to increased electron densities in bond, valence, and the outer van der Waals regions where these effects are stronger for SIC-S exchange. Despite these differences, the calculated difference densities suggest that the HF, SIC-B, and SIC-S exchange holes should possess similar delocalized structures in those situations where the reference electron is in the bonding region of N_2.

Given the delocalized structure of the SIC-DFT holes, the local character of the LDA or GGA exchange holes can only be restored if the X-SIE part is also delocalized, but in such a way that the delocalized structure of the SIC-DFT hole is annihilated. This is shown schematically in Fig. 4 for the much simpler case of the

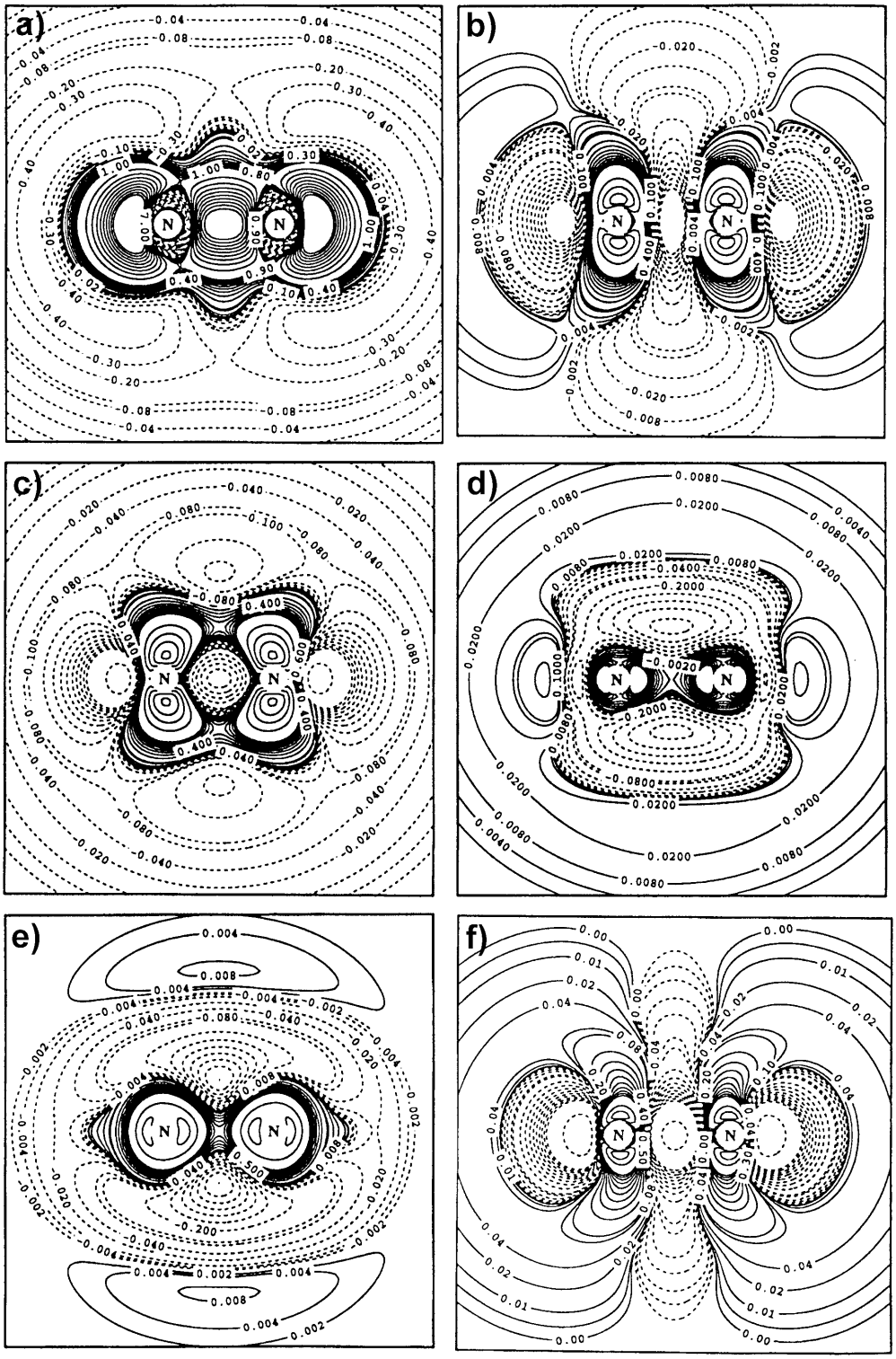

Fig. 3a–f. Contour line diagram of the difference electron density distribution $\Delta\rho(\mathbf{r}) = \rho(\text{method 1}) - \rho(\text{method 2})$ of N_2, $^1\Sigma_g^+$ calculated with the cc-pVTZ basis at the experimental geometry. The *solid* (*dashed*) contour lines are in regions of positive (negative) difference densities. The reference plane is the plane containing the two nuclei. The positions of the atoms are indicated. The contour line levels have to be multiplied by the scaling factor 0.01 and are given in e bohr^{-3}. **a** HF self-exchange assessed as the negative of Coulomb self-repulsion (method 1: DFT without × C method 2: Hartree), **b** SIE of B exchange (method 1: B only; method 2: B), **c** HF interelectronic exchange (method 1: HF; method 2: Hartree), **d** SIC-B–HF exchange, **e** SIC-S–HF exchange, **f** SIE of S exchange (method 1: S only; method 2: SIC-S)

H_2 molecule. The SIE part of the DFT exchange hole is obtained by subtracting the SIC-DFT hole from the DFT hole. It reveals that there will be an increased probability of finding the second electron in the vicinity of the two nuclei if the reference electron is at the bond midpoint (Fig. 4a). Similarly, if the reference electron is at the left nucleus, there will be a relatively large probability of finding the second electron at the right nucleus (Fig. 4b). Hence, the SIE part of the LDA exchange hole mimics long-range left–right electron correlation separating on the average two electrons over the distance of one or half a bond length depending on the position of the first electron. Because the pair correlation effects simulated by DFT exchange are long-range effects, their impact on the electron density distribution is significantly stronger than the impact of the short-range (dynamic) effects covered by MP2. This is shown schematically in Fig. 2.

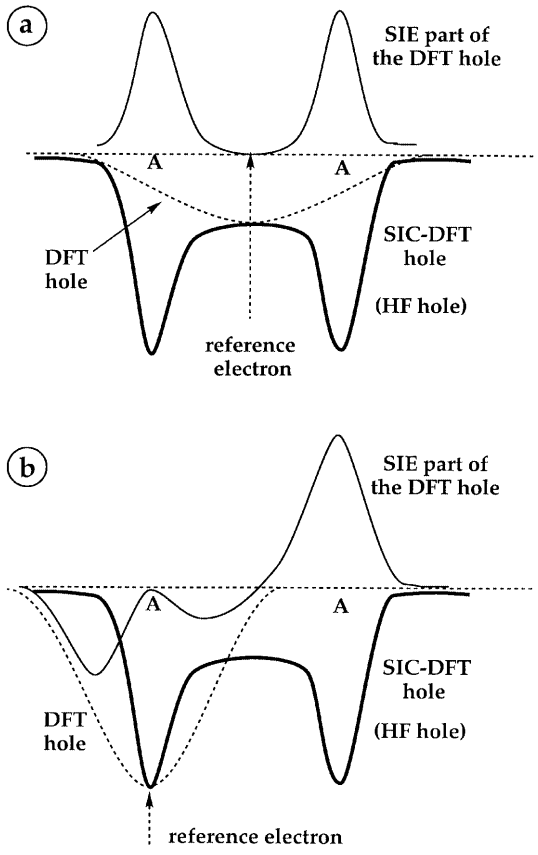

Fig. 4. Schematic representation of **a** the delocalized exchange hole of the SIC-B functional, **b** the hole associated with the SIE-B functional, and **c** the local exchange hole of a general gradient approximation functional. The reference electron is considered to be close to the right nucleus *A*

Figure 2 can be related to the stability of a restricted description of a given reference system, for example, the dissociation of N_2,[1] $^1\Sigma_g^+$. The stability parameter, λ, is listed in Table 1 for a number of XC functionals at $r(\mathrm{NN}) = 1.6$ Å, which is close but beyond the internuclear distance, at which the RDFT and UDFT dissociation curves bifurcate. The more negative λ is, the less stable is the XC functional. According to the values of Table 1, the following order of stability is obtained for the XC functionals investigated: SPL > SVWN > SVWN5 > BPL > BP86 > BLYP > PW91PW91 > BPW91 > S only > B only > B3LYP > B3PW91 > mPW91PW91 > (SIC-SVWN5 > SIC-BLYP > SIC-PW91) > HF where in the case of the SIC functionals the external stability was estimated by determining the distance r_b(NN), at which the RDFT and the UDFT solution bifurcate. Similar orders of stability were also found for other molecular systems: LDA functionals are always more stable than GGA functionals and these are more stable than hybrid functionals [31]. However, within a certain group of functionals, changes in the order of stability are possible from molecule to molecule. The rule of thumb is that a method is stabler the more correlation effects it covers. This rule can be detailed in the case of a dissociating molecule by noting that the stability of the method increases in the way that more

Table 1. Properties of N_2 ($^1\Sigma_g^+$) calculated at various levels of theory. Hartree–Fock (*HF*) and density functional theory (*DFT*) calculations with Dunning's cc-pVTZ basis set [45]. Lowest eigenvalue λ at a N–N distance of 1.6 Å, equilibrium distance R_e in (Å), harmonic vibrational frequency ω_e (cm^{-1}), dissociation energy D_e (kcal/mol)

Functional	λ	R_e	ω_e	D_e
SPL	0.0027	1.096	2396	273.1
SVWN	0.0014	1.095	2408	274.2
SVWN5	−0.0044	1.096	2478	266.9
BPL	−0.0092	1.102	2336	239.7
BP86	−0.0170	1.103	2348	244.3
BLYP	−0.0193	1.103	2338	240.5
PW91PW91	−0.0200	1.101	2360	243.0
BPW91	−0.0220	1.102	2355	237.0
S only	−0.0373	1.107	2331	211.5
B only	−0.0489	1.113	2270	178.5
B3LYP	−0.0659	1.091	2452	229.5
B3PW91	−0.0690	1.091	2463	225.4
mPW1PW91	−0.0825	1.089	2488	222.4
HF	−0.2738	1.067	2733	116.4
SIC-S		1.098[a]		182.1
SIC-B		1.098[a]		144.6
SIC-PW91X		1.098[a]		162.0
SIC-SVWN5		1.098[a]		237.8
SIC-BLYP		1.098[a]		206.8
SIC-PW91PW91		1.098[a]		219.3
Exp.[a]		1.098	2359	228.4

[a] Experimental R_e and D_e values and ω_e from Huber and Herzberg [38]

left–right correlation effects are included. A particular XC functional will lead to more stability if the exchange part includes a larger number of unspecified nondynamic electron correlation effects (instability indicates a lack of nondynamic electron correlation). Hence, DFT methods, which suffer from a larger X-SIE, are more stable than either HF, low-order MP*n* methods, or DFT methods with a smaller X-SIE, simply because the SIE mimics nondynamic electron correlation. As S-exchange covers more left–right correlation than B exchange (Figs. 1f, 2), XC functionals including S exchange are more stable than GGA functionals. We conclude that the X-SIE and the number of unspecified long-range pair correlation effects it mimics, is directly responsible for the stability of an approximate XC functional. The stability is fine-tuned by the amount of dynamic electron correlation effects covered by the C functional. This conclusion leads to two additional corollaries.

1. Since the nondynamic correlation effects artificially included via the X-SIE are unspecified, they do not necessarily lead to an improved description of the dissociating molecular system.
2. If a DFT method is used that by the form of the wave function includes long-range nondynamic correlation effects, either a double counting or a suppression of nondynamic electron correlation effects may occur.

Corollary 1 can be substantiated by data obtained with the various XC functionals for the dissociating N_2 molecule. In Table 1, the calculated dissociation energies, D_e of N_2 are listed, which confirm that the greater

stability of the XC functional does not necessarily imply a better D_e value. The magnitude of the calculated D_e(XC) values decrease in the series (XC given) SVWN > SPL > SVWN5 > BP86 > PW91PW91 > BLYP > BPL > SIC-SVWN5 > BPW91 > B3LYP $\simeq$ experiment > B3PW91 > mPW91PW91 > SIC-PW91 > PW91 only > SIC-BLYP > S only > B only > HF, where the best agreement between theory and experiment is found for B3LYP, which is a XC functional with relatively low stability (see earlier). The LDA functionals exaggerate the dissociation energy by almost 40 kcal/mol, while the GGA functionals still exaggerate D_e by 10–13 kcal/mol. Similar observations have often been attributed to the fact that DFT exaggerates the strength of the chemical bond [3, 4]. More detailed analysis has stressed that the exchange hole in the case of an atom is localized and, therefore, the DFT description is adequate for the atom; however, for a molecule the local character of the exchange hole leads to an additional admixture of long-range nondynamic electron correlation effects and, by this, to an unbalanced description of the molecule, enhancing its stability inadequately. Hence, the greater stability of an X or XC functional indicates deficiencies when describing bond parameters, for example, bond dissociation energies. SIC-DFT, although much less stable than DFT, approaches the performance of HF, which can be explained by the fact that long-range nondynamic electron correlation is no longer covered by the X-SIC functional. The best performance is provided by the B3LYP hybrid functional, which perfectly reproduces the experimental D_e value of N_2. Of course, this is due to the fact that B3LYP was calibrated against experimental data; however, the calibration was guided by the objective to minimize the SIE and, by this, the amount of unspecified nondynamic correlation, while keeping at the same time some of the latter effects. In this way, the hybrid functionals perform much better than GGA functionals.

4 Can DFT lead to a double counting of nondynamic correlation effects?

If broken-symmetry (BS) UDFT calculations are carried out for a dissociating molecule such as N_2 or any other system with multiconfigurational character, a double counting of nondynamic electron correlation could be possible as both the X functional and the form of the UDFT wave function introduce long-range left–right correlation effects. For the purpose of setting up the BS-UDFT wave function of the dissociating molecule, an initial guess is constructed by mixing the highest occupied (HO) molecular orbital and the lowest unoccupied (LU) molecular orbital of the closed-shell RDFT solution.

$$\Psi_{\text{open}}^{\text{BS-U}} = |\psi_r \overline{\psi_s}\rangle \quad , \tag{5a}$$

where

$$\psi_r = \cos\theta\ \psi_{\text{HO}} + \sin\theta\ \psi_{\text{LU}} \quad ,$$
$$\psi_s = \cos\theta\ \psi_{\text{HO}} - \sin\theta\ \psi_{\text{LU}}$$

and where the orbital rotation angle θ is optimized during the SCF iterations. The resulting orbitals ψ_r and ψ_s are the localized counterparts of ψ_{HO} and ψ_{LU}, respectively. Using Eq. (5), the open-shell part, $\Psi_{\text{open}}^{\text{BS-U}}$, of the BS-UDFT wave function can be written in the form of Eq. (6).

$$\Psi_{\text{open}}^{\text{BS-U}} = \cos^2\theta\ |\psi_{\text{HO}}\overline{\psi_{\text{HO}}}\rangle - \sin^2\theta\ |\psi_{\text{LU}}\overline{\psi_{\text{LU}}}\rangle + \sqrt{2}\cos\theta\sin\theta\ |\psi_{\text{HO}}\overline{\psi_{\text{LU}}}\rangle^T \quad . \tag{6}$$

Hence, the BS-UDFT state is a mixture of the $|\psi_{\text{HO}}\overline{\psi_{\text{HO}}}\rangle$ and $|\psi_{\text{LU}}\overline{\psi_{\text{LU}}}\rangle$ singlet states and the $|\psi_{\text{HO}}\overline{\psi_{\text{LU}}}\rangle$ ($M_S = 0$) triplet state. The spin symmetry is broken. With respect to spatial symmetry, the BS-UDFT reference state does not belong to any irreducible representation but is part of a reducible representation that covers the symmetries of the singlet and the corresponding triplet state of the dissociating molecule. The BS-UDFT wave function (Eq. 6) has two-configurational character similar to that of the generalized valence bond approach for one electron pair [54]. It introduces long-range left–right correlation as can be seen from Fig. 5a, which gives the difference density distribution ρ(BS-UBLYP)$-$ ρ(RBLYP) for the dissociating N_2 molecule at r(NN) = 1.6 Å. If a BS-UDFT calculation is carried out with, for example, the GGA functional BLYP, long-range dynamic electron correlation effects are included once via B exchange and once via the two-configurational form of the wave function of Eq. (6). One could argue that this leads to double counting of nondynamic electron correlation and exaggerated stability of the dissociating molecule relative to the separated fragments (240.5 kcal/mol, Table 1). To clarify this question, we consider first SIE and correlation effects covered by hybrid functionals.

As shown previously RDFT solutions obtained with hybrid functionals are found to be less stable than those obtained with GGA functionals, for example, the RB3LYP calculation of the dissociating N_2 molecule is less stable than the RBLYP calculation. Hybrid functionals were constructed to compensate some of the shortcomings of approximate GGA functionals [13]. By mixing in about 20% of exact exchange, part of the X-SIE is corrected and some of the long-range correlation effects are annihilated. This can be made visible by comparing the B3LYP with the BLYP and the SIC-BLYP electron density distribution of the N_2 molecule at equilibrium (Fig. 5d–f). Relative to BLYP (Fig. 5d), the B3LYP density indicates a considerable reduction of long-range left–right and other pair correlation effects. There is more density in the bond and lone-pair regions and less in the valence and van der Waals regions (Fig. 5d), which is similar to the changes found for the difference density ρ(SIC-BLYP)$-\rho$(BLYP) (Fig. 5e). However, relative to the SIC-BLYP density, which no longer includes any nondynamic pair correlation effects, B3LYP still covers a considerable number of nondynamic left–right and in–out correlation effects (Fig. 5f).

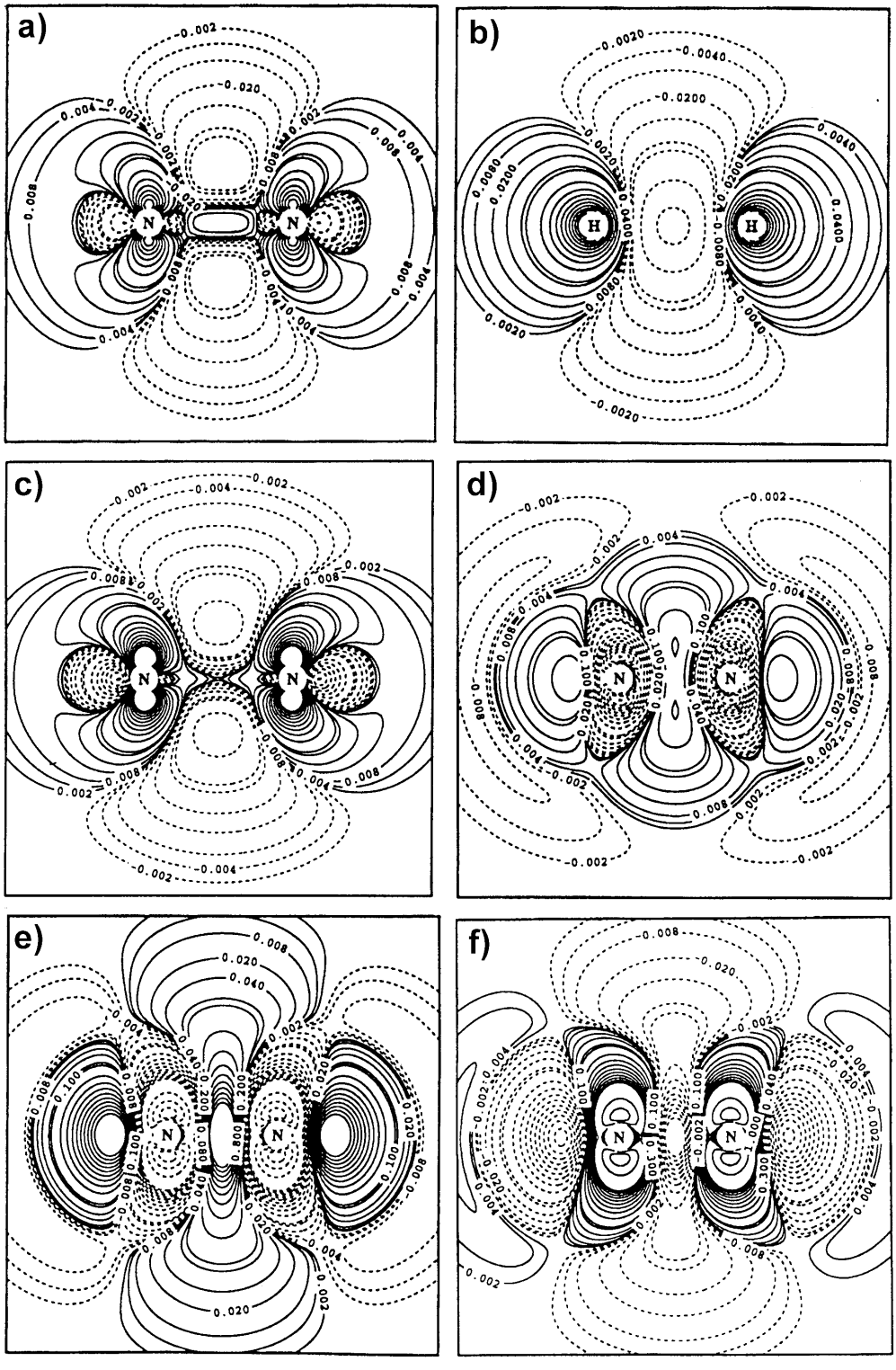

Fig. 5a–f. Contour line diagram of the difference electron density distribution $\Delta\rho(\mathbf{r}) = \rho(\text{method1}) - \rho(\text{method 2})$ of N_2,$^1\Sigma_g^+$ and H_2,$^1\Sigma_g^+$ calculated with the cc-pVTZ basis. The *solid* (*dashed*) contour lines are in regions of positive (negative) difference densities. The reference plane is the plane containing the nuclei. The positions of the atoms are indicated. The contour line levels have to be multiplied by the scaling factor 0.01 and are given in e bohr^{-3}. **a** N_2,$^1\Sigma_g^+$ at 1.6 Å: UBLYP–RBLYP. **b** H_2,$^1\Sigma_g^+$ at 1.8 Å: UBLYP–RBLYP. **c** N_2,$^1\Sigma_g^+$ at 1.7 Å: (UB3LYP–RB3LYP) – (UBLYP–RBLYP), **d** B3LYP–BLYP, **e** SIC-BLYP–BLYP, **f** B3LYP–SIC-BLYP

If there is any double counting of nondynamic electron correlation effects, this should be considerably larger for BLYP (GGA functionals) than for B3LYP (hybrid functionals). In this case, the difference density plot $\Delta(\mathbf{r}) = [\rho(\text{UB3LYP}) - \rho(\text{RB3LYP})] - [\rho(\text{UBLYP}) - \rho(\text{RBLYP})]$ should indicate a decrease rather than an increase of left–right and other pair correlation effects. We generated these plots for increasing r(NN) (Fig. 5c: $r(\text{NN}) = 1.7$ Å) and found that in all cases $\Delta(\mathbf{r})$ suggests larger pair correlation effects for the hybrid rather than the GGA functional. In addition, the calculated natural orbital occupation numbers (NOON), which provide a measure of the two-configurational character of the BS-UDFT wave function, are always larger for the LUMO of the UB3LYP than the UBLYP calculation (Table 2), indicating that the hybrid functional yields larger two-

Table 2. Biradical character, χ, and natural orbital occupation number (*NOON*) of N_2 ($^1\Sigma_g^+$) calculated at various distances, *R*, with BLYP and B3LYP. DFT calculations with Dunning's cc-pVTZ basis set [45]. The HOMO corresponds to the $1\pi_u$ orbital; the LUMO to the $1\pi_g$ orbital

	BLYP	B3LYP
$R = 1.6$ Å		
$\langle S^2 \rangle$	0.447	1.075
NOON($1\pi_u$)	1.883	1.686
NOON($1\pi_g$)	0.117	0.313
χ (%)	11.7	31.3
$R = 1.7$ Å		
$\langle S^2 \rangle$	0.929	1.423
NOON($1\pi_u$)	1.738	1.557
NOON($1\pi_g$)	0.262	0.442
χ (%)	26.2	44.2
$R = 2.0$ Å		
$\langle S^2 \rangle$	1.840	2.183
NOON($1\pi_u$)	1.406	1.293
NOON($1\pi_g$)	0.594	0.707
χ (%)	59.4	70.7

configurational character of the wave function. Similar observations are made when using methods such as restricted ensemble KS (REKS) DFT, [55] which include multiconfigurational methods in a more direct way: the NOON values obtained for the REKS/B3LYP calculation indicate more multiconfigurational character than the NOON values of the REKS/BLYP calculation [56].

Actually this result is reasonable because the method, which includes more nondynamic correlation effects in an unspecified way (e.g. BLYP) is more stable, has a lower need for a multiconfigurational treatment, and, accordingly, leads to a smaller HOMO–LUMO mixing when setting up the BS-UDFT wave function or reduced mixing of active orbitals in the case of a REKS calculation. The amount of nondynamic electron correlation covered by the exchange functional suppresses the multiconfigurational character introduced by the form of the wave function and by this double counting of nondynamic correlation effects does not occur.

Hence, it remains to be clarified whether it is of advantage to include nondynamic electron correlation via the exchange functional or via the wave function. Clearly, the first choice is more economical but suffers from the fact that an account of nondynamic electron correlation in an unspecified way cannot guarantee an accurate description of a given molecular system with distinct multiconfigurational character. In the case of BS-UDFT or REKS calculations, nondynamic electron correlation is included in a system-characteristic fashion via the form (and energy) of the frontier or active orbitals. Hence, the latter methods should always lead to more accurate descriptions for multireference problems as is amply documented in the literature (for the pitfalls when using BS-UDFT, see Ref. [57]).

In view of these arguments, it is a contradiction in itself to carry out BS-UDFT or REKS calculations with a GGA functional such as BLYP. In this case, specific nondynamic correlation effects one wants to include are suppressed by unspecified nondynamic correlation effects already included by the GGA exchange functional. Hence, one reduces the efficiency of multiconfigurational DFT and carries out DFT at high cost but with little chance of improving the accuracy of the DFT description. BS-UDFT, REKS, etc. should always use hybrid functionals such as B3LYP because only the latter guarantee maximum efficiency and a description of the multiconfigurational system preferentially by specific rather than unspecified nondynamic correlation effects.[1] This is directly reflected by the dissociation energies listed in Table 1 [B3LYP leads to a D_e(NN) value of 229.5 kcal/mol in close agreement with the experimental value of 228.4 kcal/mol [38]] and the N_2 dissociation curves shown in Fig. 6.

These consideration will not play any role if correlation functionals are combined with HF, GVB [58], or CASSCF [59] exchange since at these levels of theory the exchange hole adopts its correct form.

5 Is there a need for a generally applicable SCF-SIC-DFT method?

The SCF-SIC-DFT method used in this work is expensive relative to standard DFT and suffers from theoretical deficiencies as pointed out in Sect. 2. One could argue that a suppression of all unspecified nondynamic correlation effects and a correct description of the exchange hole provides a better basis for any multiconfigurational DFT, which includes nondynamic correlation effects in a specific and, by this, more effective way (however, losing by this, the conceptual simplicity and low cost of standard DFT).

SIC-DFT methods apart from special cases lead mostly to a deterioration of results as is reflected by the D_e values of Table 1: they are either too large (SIC-SVWN5) or too small (SIC-BLYP and SIC-PW91). It has also been observed in other investigations that SIC-DFT descriptions of normal closed-shell molecules do not offer much improvement relative to standard DFT methods [25]. This reflects simply the fact that the XC functionals used in the SIC-DFT calculations were optimized with rather than without the SIE. Hence, SIC-DFT can only offer an improved performance if XC functionals are reoptimized under SIE-free conditions.

As reflected by the N_2 dissociation potentials shown in Fig. 6, SIC-RBLYP suffers from similar deficiencies as RHF. The method is less stable than RBLYP (early bifurcation point, Fig. 6) and the potential increases steeply for increasing *r*(NN). The SIC-UBLYP potential is similarly curved as the corresponding full configuration interaction (FCI) potential curve, however as mentioned earlier the D_e value calculated (206.7 kcal/mol, Table 1) is 22 kcal/mol too small. The best agreement with the FCI potential curve [60] is obtained with the UB3LYP description, while UBLYP or UPW91PW91 deviate from the FCI curve.

[1] The B3LYP functional is less stable and indicates in this way the need for nondynamic electron correlation effects, which are specifically introduced via the form of the wave function.

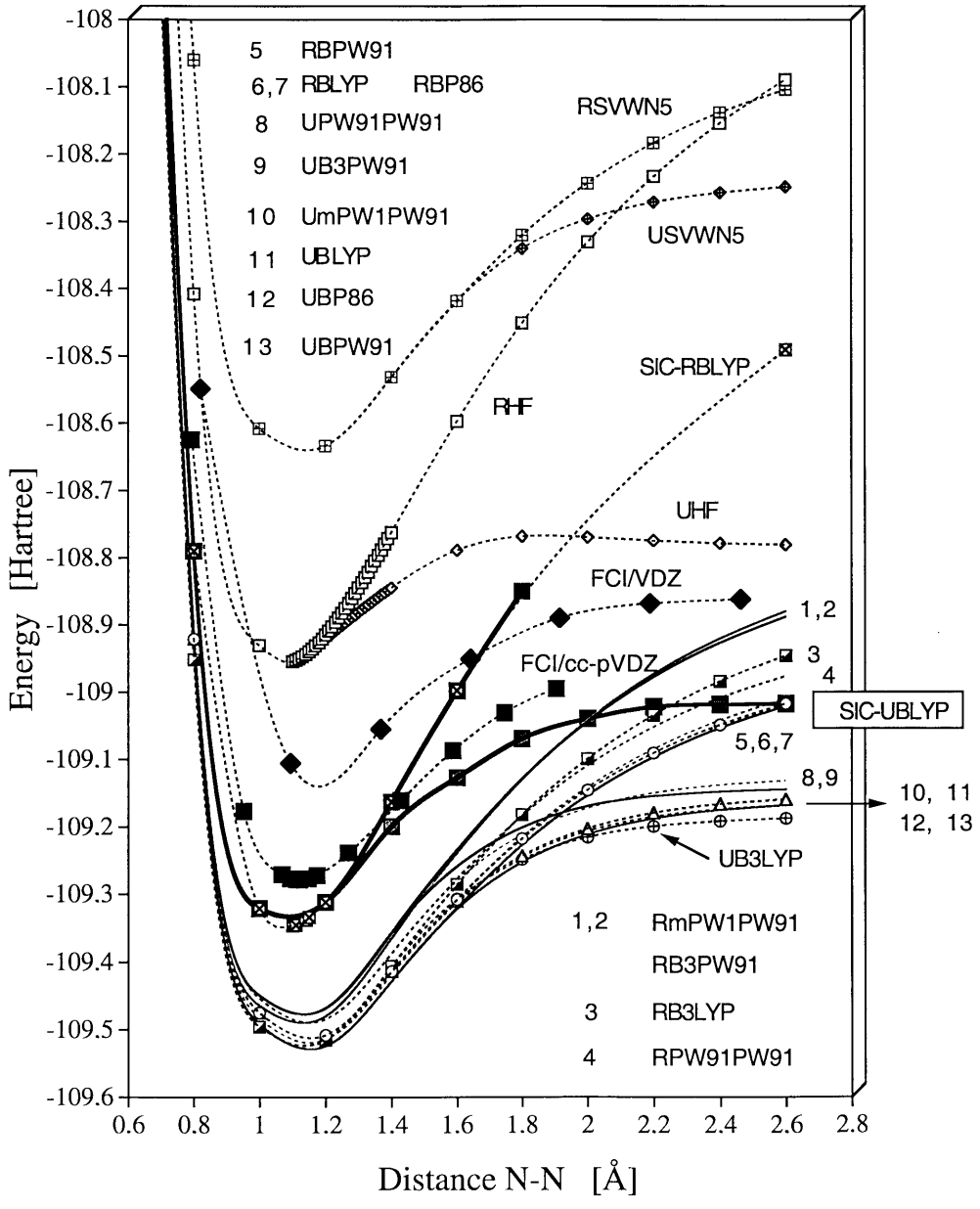

Fig. 6. Dissociation curves of N_2, $^1\Sigma_g^+$ as obtained with different WFT and DFT method

These arguments suggest that a useful SIC-DFT method must restore the computational simplicity of standard DFT. Simpler SCF-SIC-DFT methods have been suggested [61], however these are still more expensive than perturbational SIC-DFT is. For example, one can refrain from mixing occupied with occupied orbitals in the SCF-SIC-DFT procedure (which actually helps to avoid breaking the molecular symmetry); however, the energy minimum in the SIC-DFT minimization is not obtained and the SIE is underestimated. There is need for SIE-free XC functionals constructed in a similar way as the LYP correlation functional [10]. SIE-free XC functionals would be the appropriate functionals for use in connection with BS-UDFT, REKS, or any other multiconfigurational DFT; however, the best choice of an XC functional would be one that excludes SIE and includes long-range correlation effects in a specific way. The present analysis is considered to provide some of the knowledge needed for designing such functionals.

5 Conclusions

The SIE of commonly used X functionals converts the delocalized SIC-DFT exchange hole to the localized, spherically symmetric form of the DFT exchange hole. In this way, features of the electronic structure contained in the SIC-DFT exchange hole are lost, for example, important exchange delocalization effects can no longer be described. The SIE part of the DFT hole, however, mimics long-range (nondynamic) electron correlation effects, which increase the stability of the RDFT solution. The SIE is larger for LDA than for GGA functionals and, accordingly, the former simulate more nondynamic electron correlation effects and become

more stable. The order of the stabilities of commonly used XC functionals reflects directly the magnitude of their SIEs and the nondynamic correlation effects mimicked.

BS-UDFT, REKS, and other multiconfigurational DFT calculations introduce nondynamic electron correlation effects via the form of the wave function. These effects, however, will be suppressed if the exchange functional already covers a considerable number of nondynamic correlation effects in an unspecified way, thus reducing the effectiveness of the multiconfigurational DFT calculation; hence, the latter should be preferentially done with B3LYP or other hybrid functionals rather than with GGA functionals such as BLYP. The instability of the hybrid functionals is not a reason against their use, on the contrary it can be considered as useful indicator for the need of system-specific nondynamic electron correlation effects that are best introduce via multiconfigurational DFT.

Acknowledgements. This work was supported financially by the Swedish Natural Science Research Council (NFR). The calculations were done on the supercomputers of the Nationellt Superdatorcentrum (NSC), Linköping, Sweden. D.C. and E.K. thank the NSC for a generous allotment of computer time.

References

1. Hohenberg P, Kohn W (1994) Phys Rev B 136: 864
2. Kohn W, Sham L (1965) Phys Rev A 140: 1133
3. (a) Parr RG, Yang W (1989) International series of monographs on chemistry 16: Density-functional theory of atoms and molecules. Oxford University Press, New York; (b) Labanowski JK, Andzelm JW (eds) (1990) Density functional methods in chemistry. Springer, Berlin Heidelberg New York; (c) Seminario JM, Politzer P (eds) (1996) Theoretical and computational chemistry, vol 2: Modern density functional theory – a tool for chemistry. Elsevier, Amsterdam; (d) Chong DP (ed) (1995) Recent advances in computational chemistry, vol 1. Recent advances in density functional methods, part II. World Scientific, Singapore; (e) Dobson JF, Vignale G, Das MP (eds) (1997) Electronic density functional theory, recent progress and new directions. Plenum, New York; (f) Löwdin P-O (ed) (1999) Advances in quantum chemistry, vol 33. Density functional theory. Academic, New York
4. (a) Laird BB, Ross RB, Ziegler T (eds) (1996) Chemical applications of density functional theory. ACS symposium series 629. American Chemical Society, Washington, DC; (b) Joubert D (ed) (1997) Lecture notes in physics. Density functionals: Theory and applications. Springer, Berlin Heidelberg New York; (c) Gill P (1998) In: Schleyer PvR, Allinger NL, Clark T, Gasteiger J, Kollman PA, Schaefer HF III, Schreiner PR (eds) Encyclopedia of computational chemistry, vol 1. Wiley Chichester, p 678, and references therein; (d) Kraka E, Sosa CP, Cremer D (1996) Chem Phys Lett 260: 43; (e) Gutbrod R, Kraka E, Schindler RN, Cremer D (1997) J Am Chem Soc 119: 7330; (f) Gräfenstein J, Cremer D, Kraka E (1998) Chem Phys Lett 288: 593; (g) Cremer D, Kraka E, Szalay PG (1998) Chem Phys Lett 292: 97; (h) Gräfenstein J, Hjerpe AM, Kraka E, Cremer D (2000) J Phys Chem A 104: 1748; (i) Kraka E, Cremer D (2000) J Am Chem Soc 122: 8245
5. Slater J (1951) Phys Rev 81: 385
6. Vosko SH, Wilk L, Nusair M (1980) Can J Phys 58: 1200
7. Perdew JP, Zunger A (1981) Phys Rev B 23: 5048
8. Becke AD (1988) Phys Rev A 38: 3098
9. Perdew JP (1986) Phys Rev B 33: 8822
10. Lee C, Yang W, Parr RG (1988) Phys Rev B 37: 785
11. (a) Perdew JP (1991) In: Ziesche P, Eschrig H (eds) Electronic structure of solids '91. Akademie-Verlag, Berlin, p 11; (b) Perdew JP, Wang Y (1992) Phys Rev B 45: 13244; (c) Perdew J P, Wang Y (1992) Phys Rev B 45: 13244
12. Becke AD (1993) J Chem Phys 98: 1372
13. Becke AD (1993) J Chem Phys 98: 5648
14. Becke AD (1996) J Chem Phys 104: 1040
15. Adamo C, Barone V (1997) Chem Phys Lett 272: 242
16. Adamo C, Barone V (1998) J Chem Phys 108: 664
17. Becke AD (2000) J Chem Phys 112: 4020, and references therein
18. (a) Perdew JP, Kurth S, Zupan A, Blaha P (1999) Phys Rev Lett 82: 2544; (b) Becke AD (2000) J Chem Phys 112: 4020, and references therein
19. Fermi E, Amaldi E (1934) Accad Ital Rome 6: 117
20. (a) Lindgren I (1971) Int J Quantum Chem Symp 5: 411; (b) Perdew JP (1979) Chem Phys Lett 64: 127
21. (a) Perdew JP (1984) In: Avery J, Dahl JP (eds) Local density approximations in quantum chemistry and solid state physics. Plenum, New York, pp: (b) Perdew JP, Ernzerhof M (1998) In Dobson JF, Vignale G, Das MP (eds) Electronic density functional theory: Recent progress and new directions. Plenum New York, p 31
22. Perdew JP (1990) Adv Quantum Chem 21: 113
23. (a) Lundin U, Eriksson O (2001) Int J Quant Chem 81: 247; (b) Biagini M (1994) Phys Rev B 49: 2156; (c) Svane A (1995) Phys Rev B 51: 7924; (d) Biagini M (1995) Phys Rev B 51: 7927
24. (a) Harrison JG, Heaton R, Lin CC (1983) J Phys B At Mol Opt Phys 16: 2079; (b) Pederson MR, Heaton RA, Lin CC (1984) J Chem Phys 80: 1972; (c) Pederson MR Lin CC (1988) J Chem Phys 88: 1807
25. Goedecker S, Umriger CJ (1977) Phys Rev A 55: 1765
26. (a) Guo Y, Whitehead MA (1991) J Comput Chem 12: 803; (b) Chermette H, Ciofini I, Mariotti F, Daul C (2001) J Chem Phys 114: 1447
27. (a) Li Y, Krieger JB (1990) Phys Rev A 41: 1701; (b) Gill PMW, Johnson BG, Gonzales CA, Pople JA (1994) Chem Phys Lett 221: 100; (c) Whitehead MA, Suba S (1995) In: Chong DP (ed) Recent advances in computational chemistry, vol 1. Recent advances in density functional methods, part I. World Scientific, Singapore, p 53; (d) Chen J, Krieger JB, Li Y (1996) Phys Rev A 54: 3939; (e) Garza J, Nichols JA, Dixon DA (2000) J Chem Phys 112: 7880; (f) Garza J, Nichols JA, Dixon DA (2000) J Chem Phys 113: 6029; (g) Garza J, Vargas R, Nichols JA, Dixon DA (2001) J Chem Phys 114: 639
28. Polo V, Kraka E, Cremer D Mol Phys in press
29. Seeger R, Pople JA (1977) J Chem Phys 66: 3045
30. Bauernschmitt R, Ahlrichs R (1996) J Chem Phys 104: 9047
31. Gräfenstein J, Hjerpe AM, Kraka E, Cremer D (2000) J Phys Chem A 104: 1748
32. (a) Schreiner PR, Prall M (1999) J Am Chem Soc 121: 8615 (b) Prall M, Wittkopp A, Schreiner PR (2001) J Phys Chem A 105: 9265
33. Cramer CJ, Squires RR (1999) Org Lett 1: 215
34. Kraka E, Gauss J, Cremer D (1991) J Mol Struct (THEOCHEM) 234: 95
35. Gauss J, Cremer D (1992) Adv Quantum Chem 23: 205
36. Cremer D (2001) Mol Phys 99: 0000
37. He Y, Gräfenstein J, Kraka E, Cremer D (2000) Mol Phys 98: 1639
38. (a) Huber KP, Herzberg GH (1979) Molecular spectra and molecular constants of diatomic molecules. Van Nostrand-Reinhold, New York; (b) Orlov ML, Ogilvie JF, Nibler JW (1997) J Mol Spectrosc 185: 128
39. Møller C, Plesset MS (1934) Phys Rev 46: 618
40. Cremer D (1998) In: Schleyer PvR, Allinger NL, Clark T, Gasteiger J, Kollman PA, Schaefer HF III, Schreiner PR (eds) Encyclopedia of computational chemistry, vol 1. Wiley Chichester, p 1706
41. (a) Crawford TD, Schaefer HF III (2000) In: Lipkowitz KB, Boyd DB (eds) Reviews in computational chemistry, vol 14.

Verlag Chemie, Weinheim, p 33; (b) Gauss J (1998) In: Schleyer PvR, Allinger NL, Clark T, Gasteiger J, Kollman PA, Schaefer HF III, Schreiner PR (eds) Encyclopedia of computational chemistry, vol 1. Wiley Chichester, p 615
42. (a) Bartlett RJ, Stanton JF (199) In: Lipkowitz KP, Boyd DB (eds) Reviews in computational chemistry, vol 5. Verlag Chemie, Weinheim, p 65; (b) Cremer D, He Z (1997) In: Calais J-L, Kryachko E (eds) Conceptual perspectives in quantum chemistry, vol III. Kluwer, Dordrecht, p 239
43. Purvis GD III, Bartlett RJ (1982) J Chem Phys 76: 1910
44. Raghavachari K, Trucks GW, Pople JA, Head-Gordon M (1989) Chem Phys Lett 157: 479
45. Dunning TH Jr (1989) J Chem Phys 99: 1007
46. Kraka E, Gräfenstein J, Gauss J, Polo V, Reichel F, Olsson L, Konkoli Z, He Z, Cremer D (2001) COLOGNE2001. Göteborg University, Göteborg
47. Frisch MJ, Trucks GW, Schlegel HB, Scuseria GE, Robb MA, Cheeseman JR, Zakrzewski VG, Montgomery JA Jr, Stratmann RE, Burant JC, Dapprich S, Millam JM, Daniels AD, Kudin KN, Strain MC, Farkas O, Tomasi J, Barone V, Cossi M, Cammi R, Mennucci B, Pomelli C, Adamo C, Clifford S, Ochterski J, Petersson GA, Ayala PY, Cui Q, Morokuma K, Malick DK, Rabuck AD, Raghavachari K, Foresman JB, Cioslowski J, Ortiz JV, Stefano BB, Liu G, Liashenko A, Piskorz P, Komaromi I, Gomperts R, Marti RL, Fox DJ, Keith T, Al-Laham MA, Peng CY, Nanayakkara A, Gonzalez C, Challacomb M, Gill PMW, Johnson B, Chen W, Wong MW, Andres JL, Gonzalez C, Head-Gordon M, Replogle ES, Pople JA (1998) Gaussian98, revision A3. Gaussian, Pittsburgh, Pa
48. (a) Stanton JF, Gauss J, Watts JD, Lauderdale WJ, Bartlett RJ (1992) ACES II, quantum theory project. University of Florida; (b) Stanton JF, Gauss J, Watts JD, Lauderdale WJ, Bartlett RJ (1992) Int J Quant Chem Symp 26: 879
49. (a) He Z, Cremer D (1991) Int J Quantum Chem Symp 25: 43; (b) He Z, Cremer D (1993) Theor Chim Acta 85: 305
50. Slater JC (1974) The self-consistent field for molecules and solids. McGraw-Hill, New York
51. Becke AD (1995) In: Yarkony DR (ed) Advanced series in physical chemistry, vol 2. Modern electronic structure theory, part II. World Scientific, Singapore, p 1022
52. Gritsenko OV, Ensing B, Schipper PRT, Baerends EJ (2000) J Phys Chem A 104: 8558
53. Schipper PRT, Gritsenko OV, Baerends EJ (1998) Phys Rev A 57: 1729
54. Bobrowicz FW, Goddard WA III (1977) In: Schaefer HF III (ed) Methods of electronic structure theory. Modern theoretical chemistry, vol 3. Plenum, New York, p 79
55. Filatov M, Shaik S (1999) Chem Phys Lett 304: 429
56. Cremer D, Filatov M, Polo V, Kraka E (2002) Int J Mol Sci to be published
57. Gräfenstein J, Kraka E, Filatov M, Cremer D Int J Mol Sci in press
58. (a) Kraka E (1992) Chem Phys 161: 149; (b) Kraka E, Cremer D, Nordholm S (1991) In: Maksic Z, Eckert-Maksic M (eds) Molecules in natural science and biomedicine. Ellis Horwood, Chichester, p 351
59. (a) Gräfenstein J, Cremer D (2000) Chem Phys Lett 316: 569; (b) Gräfenstein J, Cremer D (2000) Phys Chem Chem Phys 2: 2091
60. Larsen H, Olsen J, Jorgensen P, Christiansen O (2000) J Chem Phys 113: 6677
61. Patchkovskii S, Autschbach J, Ziegler T (2001) J Chem Phys 115: 26